The structural basis for the specificity of pyridinylimidazole inhibitors of p38 MAP kinase

Keith P Wilson*, Patricia G McCaffrey*, Kathy Hsiao, Sam Pazhanisamy, Vincent Galullo, Guy W Bemis, Matthew J Fitzgibbon, Paul R Caron, Mark A Murcko and Michael SS Su

Background: The p38 mitogen-activated protein (MAP) kinase regulates signal transduction in response to environmental stress. Pyridinylimidazole compounds are specific inhibitors of p38 MAP kinase that block the production of the cytokines interleukin-1β and tumor necrosis factor α, and they are effective in animal models of arthritis, bone resorption and endotoxin shock. These compounds have been useful probes for studying the physiological functions of the p38-mediated MAP kinase pathway.

Results: We report the crystal structure of a novel pyridinylimidazole compound complexed with p38 MAP kinase, and we demonstrate that this compound binds to the same site on the kinase as does ATP. Mutagenesis showed that a single residue difference between p38 MAP kinase and other MAP kinases is sufficient to confer selectivity among pyridinylimidazole compounds.

Conclusions: Our results reveal how pyridinylimidazole compounds are potent and selective inhibitors of p38 MAP kinase but not other MAP kinases. It should now be possible to design other specific inhibitors of activated p38 MAP kinase using the structure of the nonphosphorylated enzyme.

Address: Vertex Pharmaceuticals Incorporated, 130 Waverly Street, Cambridge, MA 02139-4211, USA.

*These authors made an equal contribution to this work

Correspondence: Michael SS Su
E-mail: su@vpharm.com

Key words: IL-1, p38 MAP kinase, pyridinylimidazole inhibitor, TNF, X-ray structure

Received: **4 April 1997**
Accepted: **6 May 1997**

Chemistry & Biology June 1997, 4:423–431
http://biomednet.com/elecref/1074552100400423

Introduction

Mammalian mitogen-activated protein (MAP) kinases are serine/threonine protein kinases that mediate intracellular signal transduction pathways [1,2]. Members of the MAP kinase family share sequence similarity and conserved structural domains, and include the extracellular-signal regulated kinases (ERKs), Jun N-terminal kinases (JNKs) and p38 kinases. ERKs are activated by mitogen and growth factors via a Ras-dependent pathway [3]. In contrast, JNKs and p38 kinases are activated in response to the pro-inflammatory cytokines tumor necrosis factor α (TNF-α) and interleukin-1 (IL-1), and by cellular stresses such as heat shock, hyperosmolarity, ultraviolet radiation, lipopolysaccharides (LPS) and inhibitors of protein synthesis [4–7]. Two MAP kinase kinases, MKK3 and MKK6, have been identified as p38-specific activating kinases that do not phosphorylate JNKs [8–10], suggesting that the activation of p38 MAP kinase is mediated by a distinct but parallel signaling pathway(s) to that of JNKs.

The first p38 MAP kinase (also termed p38/p40/RK/SAPK/CSBP) was cloned following its identification as a kinase that was tyrosine-phosphorylated after stimulation of monocytes by LPS [5]. The p38 MAP kinase was later identified as the drug target for a group of pyridinylimidazole compounds that block the production of IL-1β and TNF-α from monocytes stimulated by LPS [11]. SB-203580, a 2,4,5-triarylimidazole (Figure 1; **2**), is a potent p38 MAP kinase inhibitor that is highly selective relative to other kinases, including other closely related MAP kinases [12–13]. SB-203580 has been shown to be effective in animal models of arthritis, bone resorption and endotoxin shock [14], and has proven to be a useful research tool in determining the role of the p38-mediated kinase pathway [7,15]. But, as yet, no structural studies have been reported that describe the binding and p38-selectivity of this class of compound.

The p38 MAP kinase has been implicated in the translational control of cytokine gene expression [16]. In addition, it phosphorylates and activates transcription factors ATF-2, Elk-1, CHOP-1, and MEF2C [10,17–18], indicating the involvement of p38 MAP kinase in transcriptional regulation. The p38 kinase has also been implicated in the activation of MAP-kinase-activated protein kinases (MAPKAPKs) 2 and 3 [19–20], activation of platelets [15], production of IL-6 and IL-8 [7], induction of cyclooxygenase 2 [21], and apoptosis of neuronal cells [22]. Selective modulation of p38 MAP kinase activity could therefore provide therapeutic intervention for disorders ranging from inflammatory diseases to neurodegenerative diseases.

The crystal structure of apo-, unphosphorylated p38 MAP kinase has been described [23–24]. The amino acid

Figure 1

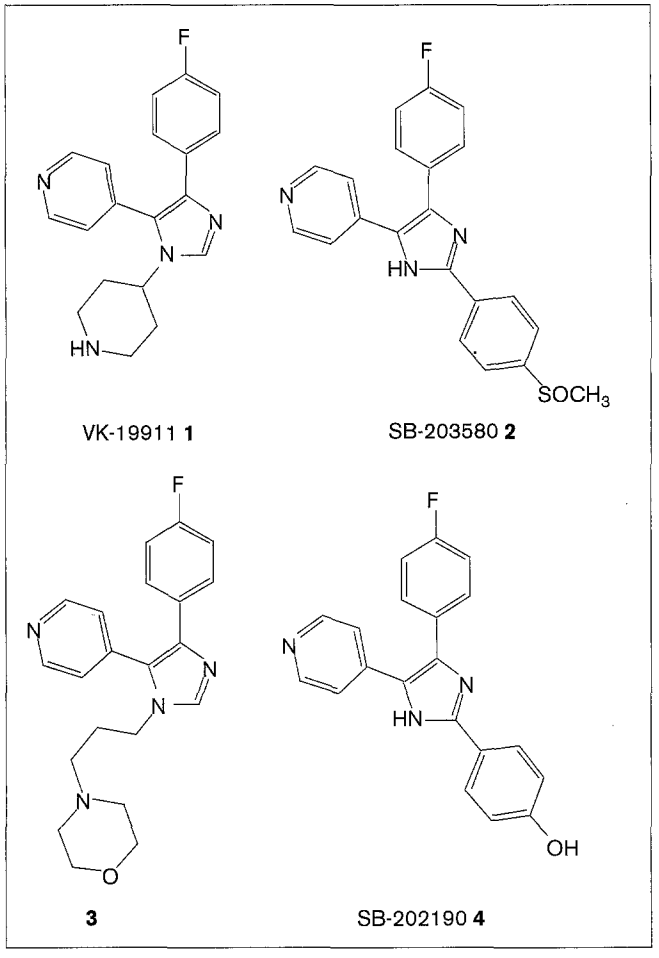

Selected pyridinylimidazole compounds. (**1**) VK-19911: 4-(4-fluorophenyl)-1-(4-piperidinyl)-5-(4-pyridyl)-imidazole. (**2**) SB-203580: a 2,4,5-triarylimidazole. (**3**) An N1-morpholinopropyl-4,5-diarylimidazole derivative. (**4**) SB-202190: a 2,4,5-triarylimidazole.

Figure 2

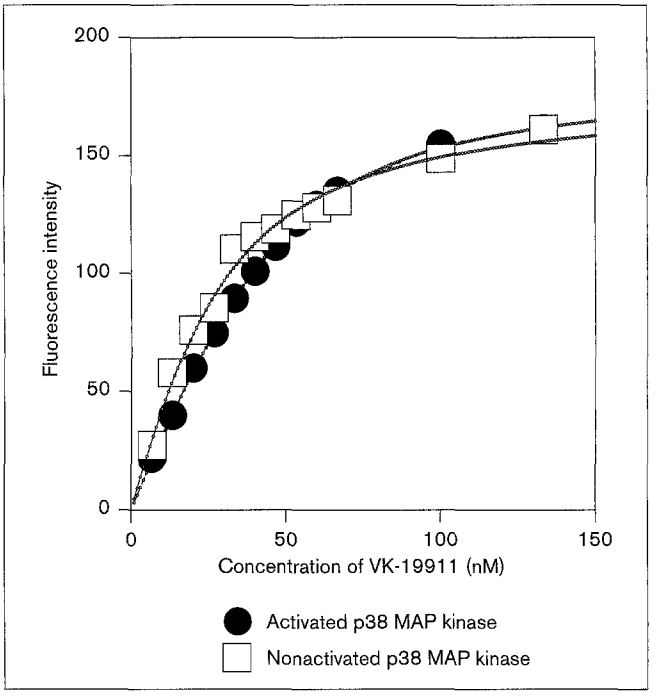

Determination of dissociation constant K_d for VK-19911 with nonactivated and activated p38 MAP kinase. Both activated (filled circles) and nonactivated (open squares) p38 MAP kinase have similar affinities for VK-19911 ($K_d = 12 \pm 1$ nM and 15 ± 5 nM, respectively). The concentration of p38 MAP kinase (activated or nonactivated) was maintained at 80 nM in 0.1 M HEPES buffer, pH 7.6, containing 10 mM magnesium chloride and 25 mM β-glycerophosphate. VK-19911 in DMSO (10 μM) was added in small aliquots. The excitation and emission wavelengths were 280 nm and 375 nm, respectively. Under the experimental conditions, DMSO did not have any significant effect on the emission signal. The emission intensities for the activated p38 MAP kinase shown in this figure were scaled down twofold from the original. The titration curves were fitted to Equation 1 (see the Materials and methods section) to obtain the dissociation constants.

sequences of p38 and ERK2 are 48% identical and their folds and topology are similar [23–25]. Enzymes in the MAP kinase family as a whole are characterized by two domains separated by a deep channel in which substrates have the potential to bind. The amino-terminal domain creates a binding pocket for the adenine ring of ATP, and the carboxy-terminal domain contains the presumed catalytic base, magnesium-binding sites, and phosphorylation lip (Thr–X–Tyr motif; see later). Here, we report the crystal structure of p38 MAP kinase bound to VK-19911 — 4-(4-fluorophenyl)-1-(4-piperidinyl)-5-(4-pyridyl)-imidazole; Figure 1; **1** — an inhibitor from the pyridinylimidazole class of compounds. X-ray diffraction data, in concert with mutagenesis results, reveal for the first time the enzyme conformational changes and amino acid contacts responsible for the selective and potent binding of the pyridinylimidazole compounds within the ATP-binding site of p38 MAP kinase.

Results and discussion

The p38 MAP kinase–inhibitor complex

VK-19911 (Figure 1; **1**) is a potent ligand for both nonphosphorylated and phosphorylated p38 MAP kinase, having similar dissociation constants with each form of the enzyme ($K_d \approx 15$ nM and 12 nM, respectively, as measured by fluorescence emission at 375 nm upon binding VK-19911 to the enzyme; Figure 2). We report the structure of nonphosphorylated p38 MAP kinase bound to VK-19911 at 2.6 Å resolution as determined by X-ray diffraction.

Electron density for the mainchain atoms of p38 MAP kinase complexed with the inhibitor VK-19911 is visible for residues 5–352, with breaks at residues 14–15, 118–122, and 170–174 (data not shown). Four residues at the amino-terminus of p38 MAP kinase, and six amino acids remaining from the thrombin cleavage site (see [23]), are not visible in the electron density map. The presence of these

Figure 3

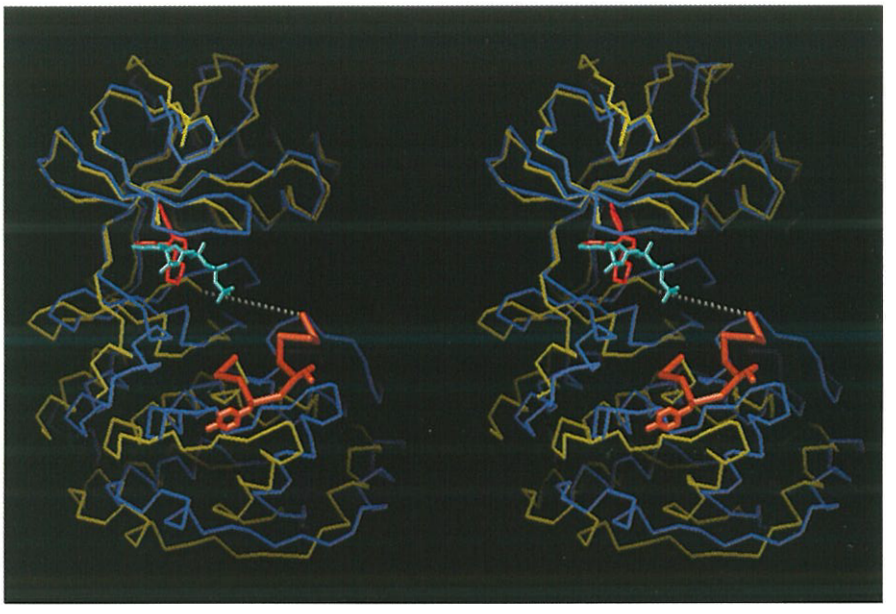

Pyridinylimidazole compounds bind in the ATP-binding site. Stereo Cα representations of the structures of p38 MAP kinase (gold) complexed with VK-19911 (red liquorice bonds) and ERK2 (dark blue) complexed with ATP (light blue liquorice bonds) are shown after superposition of their amino-terminal domains. The phosphorylation lip of p38 MAP kinase is highlighted with orange liquorice bonds. The sidechains of Thr180 and Tyr182 that become phosphorylated upon activation of p38 MAP kinase are shown. A thin dotted line connects Phe169 to Asp174 and may trace approximately the path of the disordered residues between these two amino acids. The distance between either Thr180 or Tyr182 and VK-19911 is 24 Å. Because the residues in the phosphorylation lip are quite distant from the ligand-binding site, it is expected from the structure that the activation of p38 MAP kinase should have little effect on the shape of the binding pocket and hence the affinity of p38 MAP kinase for compounds in the pyridinylimidazole class.

amino acids in the crystal structure has been confirmed by sequence analysis. Seven residues at the carboxyl terminus are also disordered. The phosphate anchor, which contains the consensus sequence Gly–X–Gly–X–X–Gly (residues 31–36 in p38 MAP kinase; data not shown), is highly mobile and these residues are also omitted from the model.

The inhibitor binds in the ATP-binding site

A comparison of the structures of the p38 MAP kinase–VK-19911 complex and the ERK2–ATP complex suggests that VK-19911 competes with ATP for binding at the active site (Figure 3). In the structure of the ERK2–ATP complex, the amide nitrogen of Met106 forms a hydrogen bond with the N1 nitrogen of the adenine ring of ATP (Figure 4a), whereas the corresponding residue in p38 MAP kinase, Met109, forms a hydrogen bond with N4 of the pyridine ring of VK-19911 (Figure 4b). In addition to the common hydrogen bond, the two ligands have comparable van der Waals contacts with surrounding residues in each complex, for example, amino acid sidechains in the ERK2 structure that make contact with ATP include Val37, Ala50, Gln103, Met106, and Asp165. In comparison, the equivalent residues in p38 MAP kinase, which include Val38, Ala51, Thr106, Met109 and Asp168, interact with at least a portion of VK-19911. These data suggest that VK-19911 is competitive with ATP in the ATP-binding pocket of p38 MAP kinase. In fact, enzymic analysis confirms that VK-19911 is competitive with ATP as an inhibitor of p38 MAP kinase (S.P., unpublished observations).

Enzyme–inhibitor interactions

We examined the conformational preferences of VK-19911 to determine the strain energy of its bound state. Our calculations indicate that the global energy-minimum structure for VK-19911 is similar to the crystallographically observed bound conformation. These findings help explain the high potency of VK-19911, because the molecule binds in the active site of p38 MAP kinase in a very low-energy conformation.

Many of the contacts between VK-19911 and p38 MAP kinase arise from the *para*-fluorophenyl ring, which is completely shielded from solvent and is within favorable van der Waals distance of the carbon atoms of ten hydrophobic residues (Val38, Ala51, Val52, Lys53, Leu75, Ile84, Leu86, Leu104, Val105 and Thr106; Figure 4b). This ring, which is a common substituent in many of the most potent pyridinylimidazole inhibitors reported [26], contributes significantly to the affinity of VK-19911 to p38 MAP kinase by burying ~180 $Å^2$ of the enzyme's surface area upon binding.

Two hydrogen bonds are formed between VK-19911 and p38 MAP kinase. The pyridine ring nitrogen accepts a proton from the backbone amide nitrogen of Met109, and the nitrogen of the piperidine ring forms a salt bridge with the sidechain carboxylate group of Asp168 (Figure 4b). Based on observations of the distance and geometry, it appears that N4 in both the pyridine and piperidine rings affords the best electrostatic interaction with p38 MAP kinase. Additional enzyme–ligand interactions include contacts between the pyridine ring and Ala51, Thr106, and His107, while the piperidine moiety interacts with Met109 and Leu167. The imidazole ring, which contacts only Lys53 and Asp168, appears to assist in the binding by positioning the piperidinyl and aryl rings.

Figure 4

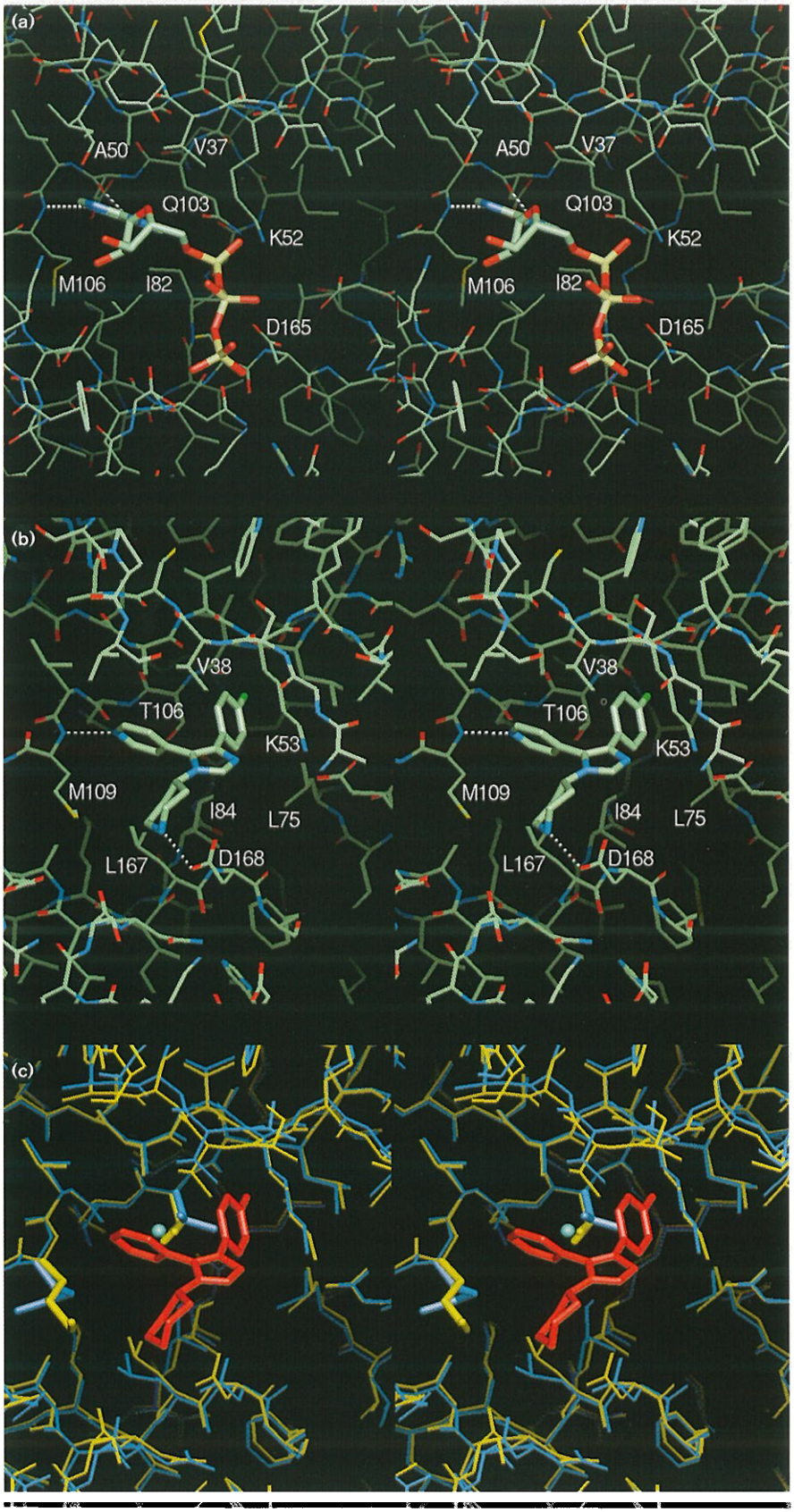

Illustrations of the active sites of ERK2 and p38 MAP kinase. **(a)** Stereo drawing of the active site of ERK2. The refined model of the ERK2–ATP complex in the region of the ATP-binding site is shown. Some of the sidechains in contact with ATP (see text) are identified (one-letter code and sequence position). Atoms in the figure are colored: carbon, yellow; nitrogen, blue; oxygen, red; and sulfur, yellow. ATP is displayed by liquorice bonds. Hydrogen bonds between ATP and ERK2 are highlighted by dashed lines. The distance between the amide-nitrogen of Met106 and N1 of the adenine ring is 3.17 Å, and the distance between the ATP adenine-ring amino group and the carbonyl oxygen of Asp104 is 3.01 Å. Water molecules in the vicinity of the ligand, and residues 30–34 of the phosphate anchor, were omitted for clarity. **(b)** Stereo drawing of the active site of p38 MAP kinase. The refined model of the complex in the region of the VK-19911-binding site is shown. Some of the sidechains in contact with the inhibitor (see text) are identified (one-letter code and sequence position). Atoms in the figure are colored: as in (a) and fluorine, green. The inhibitor is displayed in liquorice bonds. The view is approximately the same as in (a). Hydrogen bonds between the inhibitor and p38 MAP kinase are highlighted by dashed lines. The distance between the amide-nitrogen of Met109 and N4 of the pyridine ring is 2.98 Å, and the distance between N4 of the piperidine ring and the sidechain carboxylate oxygen of Asp168 is 2.85 Å. Water molecules in the vicinity of the ligand were omitted for clarity. Residues of p38 MAP kinase that have at least one atom within 4 Å of any atom in the inhibitor are: Val38, Ala51, Lys53, Ile84, Leu75, Leu86, Leu104, Val105, Thr106, His107, Leu108, Met109, Leu168, and Asp169. As in (a), the pyridine nitrogen must reside at position 4 for optimal interaction with the Met109 amide nitrogen, while simultaneously permitting the 4-fluorophenyl ring to make many van der Waals contacts. **(c)** Changes in the p38 MAP kinase active site upon ligand binding. The structure of the apo-, nonphosphorylated form of p38 MAP kinase (blue) is compared with the refined structure of the VK-19911 inhibited complex (gold). The amino acids, listed in (b), with at least one atom within 4 Å of the inhibitor were used to superimpose the two structures. The root mean square (rms) deviation of these 14 residues is 0.42 $Å^2$. The inhibitor is colored red and displayed in liquorice bonds. Liquorice bonds are also used to highlight the shift of Met109 (lower left), and the rotation about χ_1 of Thr106 (center). The water molecule bound in the apo-structure that is displaced by the γ-hydroxyl group of Thr106 upon ligand binding is highlighted as a light blue sphere. Residues 30–36 were omitted from the figure for clarity. Larger sidechains at position 106, like glutamate in ERK2 and methionine in JNK and p38γ/SAPK3, would block VK-19911 binding by occupying the space filled by the *para*-fluorophenyl ring.

Both global and local conformational changes of p38 MAP kinase accompany binding of VK-19911. The most significant movement occurs at Met109 such that C_ε shifts 7.7 Å from its location in the apo-structure (Figure 4c) to contact the piperidine ring of VK-19911. The conformational change of the methionine sidechain, which is positioned at the interface between the two domains of p38 MAP kinase (Figure 3) may be linked to a global change in the structure that occurs upon VK-19911 binding. When equivalent residues from the carboxy-terminal domain (amino acids 110–117, 123–169 and 175–318) of the apo-structure and the VK-19911-bound structure are superimposed, residues 5–60 of the amino-terminal domain are shifted by an average of 1.5 Å. Most shifts in the structure of the complex occur towards VK-19911 or towards the space vacated by the Met109 sidechain (not shown). In contrast, residues of the amino-terminal domain that are more distant from the compound and Met109 maintain their position. Thr106 also undergoes a conformational change in response to the binding of VK-19911, rotating 120° about χ_1. This movement changes the location of the Thr106 γ-hydroxyl group, which then forms a hydrogen bond with the carbonyl oxygen of Gly85 in the VK-19911-bound complex. In the apo-structure, the hydrogen bond to the carbonyl oxygen of Gly85 is formed with a water molecule, which is displaced in the inhibitor complex (Figure 4c). The 120° rotation also places the Thr106 γ-methyl group in favorable van der Waals contact with the *para*-fluorophenyl ring of VK-19911.

Inhibitor selectivity

Members of the MAP kinase family share conserved structural domains and a high degree of sequence similarity, particularly in the ATP-binding site. Not surprisingly, a number of p38 MAP kinase residues that make contact with the inhibitor are conserved among other MAP kinases. Thr106 is an exception, however, and is replaced by methionine in p38γ/SAPK3 (a newly discovered p38 homolog) [27,28] and the JNK kinases, and by glutamine in the ERK1 and ERK2 kinases. Analysis of the crystal structure suggested that substitution of Thr106 with methionine or glutamine would interfere with binding of pyridinylimidazole inhibitors by blocking access to the pocket which accepts the fluorophenyl ring. Thus, the residue corresponding to Thr106 in other MAP kinases may be a critical determinant for specificity of these compounds.

To test this hypothesis, we used site-directed mutagenesis to change Thr106 in p38 MAP kinase to methionine or alanine. Neither mutation affected the overall activity of the kinase nor its degree of activation *in vitro* by MKK6 (data not shown). Substitution of Thr106 with methionine, however, rendered the enzyme resistant to VK-19911 at a level similar to that seen for p38γ/SAPK3 (Figure 5a). Furthermore, the Thr106→Met mutant was also resistant to inhibition by the 2,4,5-triarylimidazole SB-202190 (Figure 5b), indicating that these structurally similar inhibitors are likely to bind in a similar manner. Based on the structure of p38 MAP kinase complexed with the inhibitor, replacing Thr106 with alanine would be expected to have little effect on inhibitor binding because the sidechain of alanine should not interfere with the positioning of the fluorophenyl ring. As predicted, the p38 MAP kinase Thr106→Ala mutant is as sensitive to VK-19911 or SB-202190 as the wild-type enzyme (Figure 5). These results demonstrate that Thr106 is critical for binding pyridinylimidazole compounds selectively to p38 MAP kinase, and that the presence of larger sidechains at the corresponding residue may explain the resistance of other MAP kinase homologs to these inhibitors.

Activation of p38 MAP kinase is unlikely to change its affinity for pyridinylimidazole compounds

MAP kinases reach maximum enzymic activity [29] only after phosphorylation by specific MAP kinase kinases within a Thr–X–Tyr motif, where X is Pro, Glu, or Gly for ERK, JNK, or p38 MAP kinase, respectively [1–2]. Because the Thr–X–Tyr motif is located in a surface loop near the active site, this region of the enzyme is often referred to as the phosphorylation lip or activation segment. The crystal structure of the apo-, nonphosphorylated p38 MAP kinase enzyme indicates that its phosphorylation lip includes residues 170–178, which occupy the peptide-binding channel, and residues 179–185, which include the two phosphorylation sites Thr180 and Tyr182 [30] (Figure 3). Upon phosphorylation at Thr180 and Tyr182, it is thought that a conformational change in the phosphorylation lip occurs that could influence the binding of pyridinylimidazole compounds. But the binding affinity of VK-19911 for activated p38 MAP kinase is similar to that of the nonphosphorylated enzyme ($K_d \approx 12$ nM and 15 nM, respectively; Figure 2). Inspection of the structure of the VK-19911 complex shows that the closest distance between the pyridinylimidazole compound and any residue in the phosphorylation lip is ~10 Å, and that residues Thr180 and Tyr182 are ~24 Å removed from the imidazole ring of the inhibitor (Figure 3). The large distance between the inhibitor-binding site and the phosphorylation lip reduces the likelihood that the activation of p38 MAP kinase will have a large effect on the binding affinity of VK-19911 or other pyridinylimidazole compounds.

Structure–activity relationship for pyridinylimidazole inhibitors

The complex of VK-19911 (Figure 1; **1**) bound to p38 MAP kinase provides an opportunity to rationalize published p38 MAP kinase inhibition data for other pyridinylimidazole compounds, such as the 2,4,5-triarylimidazole derivative (Figure 1; **2**) [31] and the N1-morpholinopropyl-4,5-diarylimidazole derivative (Figure 1; **3**) [32].

Figure 6 summarizes the binding features found for VK-19911. The imidazole ring of VK-19911 appears to

Figure 5

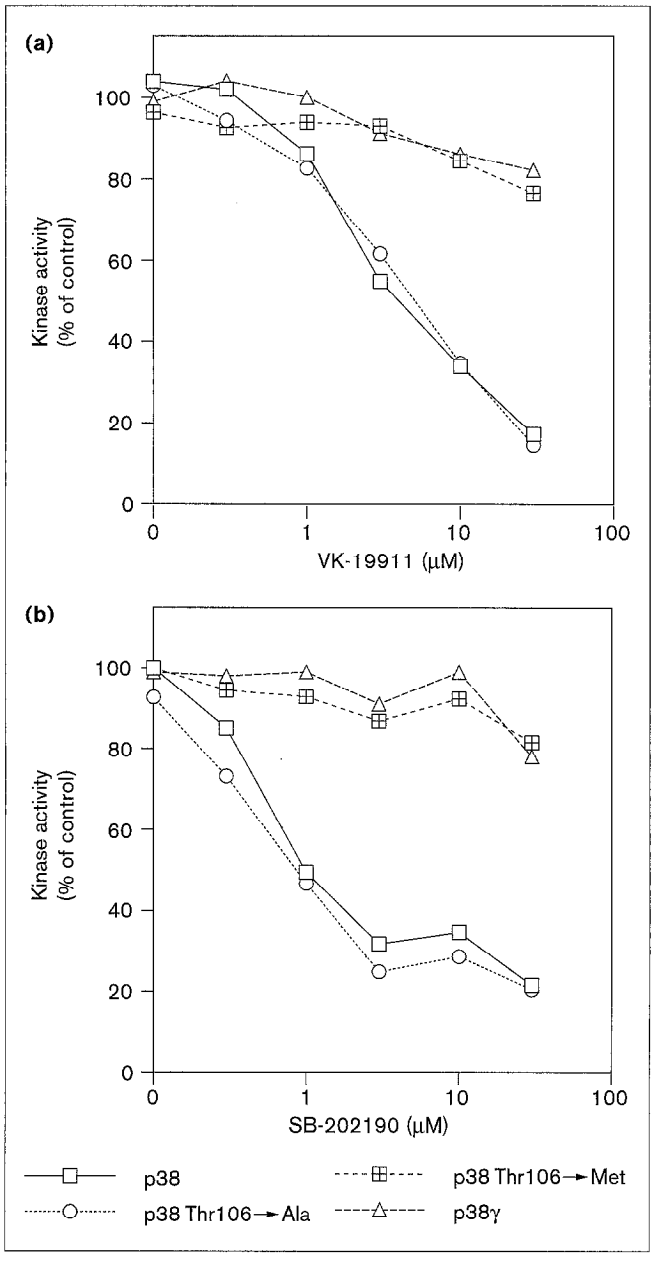

Inhibition of p38 MAP kinase, p38γ/SAPK3 and p38 MAP kinase mutants by **(a)** VK-19911 and **(b)** SB-202190. Kinase activity was measured as described in the Materials and methods section using myelin basic protein as a substrate, in the absence or presence of inhibitors at the concentrations shown. Kinase activity is expressed relative to the activity measured in the absence of inhibitor (set to 100%).

Figure 6

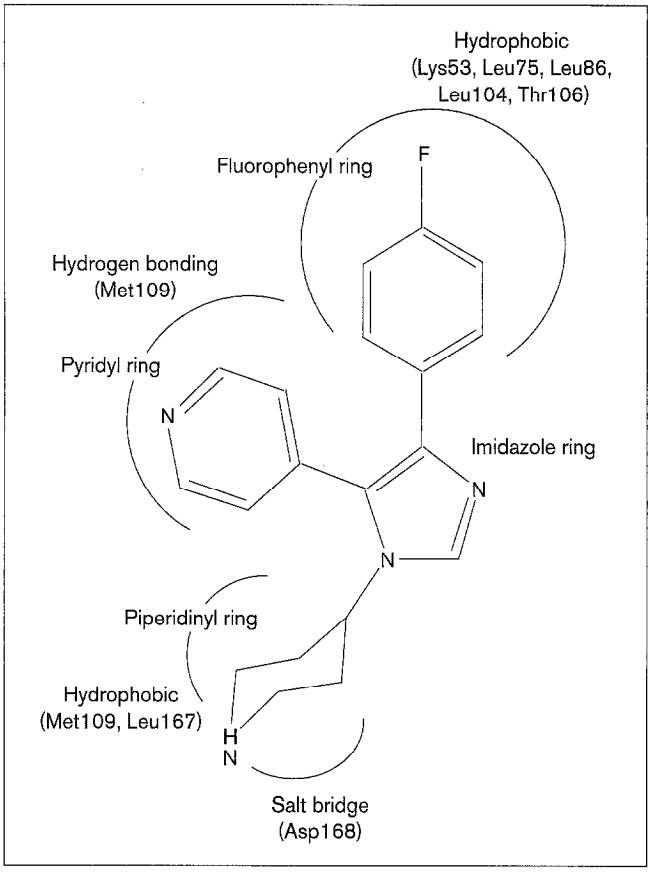

Two-dimensional schematic drawing of VK-19911 binding to p38 MAP kinase.

serve mainly as a scaffold for positioning the piperidinyl and aryl rings in place. Other studies, however, have implicated N3 in the imidazole ring as a critical determinant for the binding of pyridinylimidazole inhibitors to p38 MAP kinase [26]. The proximity of N3 to the positively charged sidechain of Lys53 suggests that a nitrogen bearing a lone pair of electrons may be required in this position to avoid a repulsive interaction, rather than to form a favorable interaction with p38 MAP kinase. Alternatively, the Lys53 sidechain may interact dynamically with the N3 lone pair either directly or through solvent.

The pyridyl ring of VK-19911 forms a hydrogen bond with the backbone carbonyl of Met109. The orientation of the 4-pyridyl ring with respect to the enzyme suggests that the 3-pyridyl and 2-pyridyl derivatives should be unable to effectively participate in this hydrogen bond and should therefore be substantially less active. In addition, replacing the pyridyl ring with a phenyl ring should reduce activity as a result of the loss of hydrogen bonding and the introduction of steric clashing. These observations are in accord with literature results [26] for compounds related to **2** and **3**.

The fluorophenyl ring of VK-19911 is buried in a hydrophobic cleft, leaving minimal space for additional substituents to the ring. The *ortho* and *meta* positions on one face of the fluorophenyl ring are sterically blocked by the backbone carbonyl of Ala51 and the sidechain of Val38, respectively, while the *para* position, as well as the *ortho*

and *meta* positions, of the opposing face of the ring appear to allow small substituents. This is consistent with literature data which show that 3,5-disubstitutions reduced the potency, whereas monosubstitution at the *meta* or *para* position increased potency of inhibitors in this class [26].

The piperidinyl ring of VK-19911 has two components of binding: hydrophobic overlap with the sidechains of Met109 and Leu167, and a salt bridge with Asp168. Interactions of C3 and C5 of the piperidin-4-yl ring with the oxygens of Asp168 are slightly repulsive. Replacement of the piperidin-4-yl moiety with 3-carboxypropyl would place the carboxyl group in direct proximity to the Asp168 sidechain, accounting for the severe loss of binding affinity of this compound [26].

Significance

We have determined the structure of p38 mitogen-activated protein (MAP) kinase bound to an inhibitor — 4-(4-fluorophenyl)-1-(4-piperidinyl)-5-(4-pyridyl)-imidazole; VK-19911 — from the pyridinylimidazole class of compounds. We found that both global and local conformational changes accompany the binding of VK-19911. By comparing the structure of the p38 MAP kinase–VK-19911 complex with that of the complex formed by the extracellular-signal regulated (ERK) kinases and ATP, it is clear that VK-19911 inhibits the p38 MAP kinase activity by blocking access of ATP to the active site. Our structural and mutagenesis data established that a single amino acid difference at residue 106 between p38 MAP kinase and other MAP kinases is sufficient to confer selectivity for VK-19911. It is thought that both the N1-substituted 4,5-diarylpyridinylimidazoles and the 2,4,5,-triarylimidazoles bind to p38 MAP kinase in a similar manner, and that all compounds in these classes inhibit p38 MAP kinase by competing with ATP. Furthermore, activation of the enzyme does not have a significant impact on the binding affinity for VK-19911, indicating that the shape of the inhibitor-binding pocket is unlikely to change upon phosphorylation of p38 MAP kinase. It is anticipated that the structure of p38 MAP kinase complexed with VK-19911 should aid the design of other highly specific inhibitors of this enzyme.

Materials and methods

Synthesis of VK-19911

The key step in the synthesis of VK-19911 uses a 1,3 dipolar cycloaddition [32,33–34] between the anion of 4-fluorophenyltolythiomethyl-isocyanide (Figure 1; **3**) [32,34] and the imine (Figure 7; **6**). Thus, **6** was prepared in one step from Boc-piperidine (Figure 7; **5**) [35] and pyridine-4-carboxaldehyde. The anion of 4-fluorophenyltolythiomethyl-isocyanide was generated by treatment with 1,5,7-triazabicylco-[4.4.0]dec-5-ene (TBD) and then condensation with imine **6** to form the Boc-protected imidazole **7** (Figure 7). Deprotection of the Boc group with 4 N HCl in dioxane afforded the desired final product.

Crystallization of p38 kinase and structure determination of VK-19911 complex

Sample preparation for crystallization of p38 MAP kinase has been published [23]. Crystals of nonphosphorylated, apo-p38 were grown by vapor diffusion as described [23]. A single crystal 0.35 mm × 0.25 mm × 0.03 mm in size was equilibrated slowly over 48 h in a buffer of 50 mM sodium HEPES, pH 7.5, 0.7 M sodium citrate, 144 mM $(NH_4)_2SO_4$, 5 mM VK-19911, and 17.5% glycerol in preparation for X-ray data collection at −169°C.

X-ray data were collected on an Raxis IIC image plate and processed and scaled using DENZO and SCALEPACK [36]. The crystals had space group symmetry $P2_12_12_1$, with unit cell dimensions a=45.36 Å, b=86.09 Å, and c=125.92 Å. The crystal exposed to the compound showed a 2.0 Å increase in cell dimension along the c-direction with respect to apo-crystals. R-merge for the data was 6.2%, with I/sig(I) = 6.0 at 2.6 Å resolution. R-merge in the highest resolution shell was 14.9%. The X-ray data comprised 13,827 unique reflections with $|F| > \sigma(F)$ derived from 42,304 intensity measurements. The data were 87% complete overall and 81% complete in the 2.72–2.60 Å resolution shell.

X-ray coordinates of apo-, nonphosphorylated p38 kinase [23] were used as a starting model for refinement of the inhibited complex (PDB accession number 1WFC). All thermal factors were set to 10.0 $Å^2$. The R-factor after rigid body refinement was 31% for data between 10–3.0 Å. The resolution of the maps and model was gradually increased to 2.6 Å resolution by cycles of model building, positional refinement, and thermal factor refinement, interspersed with torsional dynamics runs. All stages of model refinement were carried out using the XPLOR suite of programs [37]. Our current p38 model in complex with VK-19911 contains 333 protein residues, 102 water molecules, and one inhibitor molecule, and has an R-factor of 21.8% versus all data with $|F| > \sigma(F)$ between 8–2.6 Å resolution (13,336 reflections). PROCHECK and XPLOR were used to analyze the model stereochemistry. 90% of the p38 residues were located in the most favored region of the phi-psi plot, and 9% in the additional allowed regions. The model had deviations from ideal bond lengths and angles of 0.011 Å and 2.8°, respectively, and all other indications of stereochemistry were average or better then average for a structure determined at 2.6 Å resolution. No electron density was observed for p38 amino acids 1–4, 14–15, 118–122, 170–174, and 353–359 in the complex and these residues were not, therefore, included in the model. Residues Arg10, Arg149, His199 and Leu353 were modeled as alanine because the electron density for these sidechains was poor.

Expression and purification of kinases

EST clones containing the entire coding regions of human MKK6 (MKK6b) [9] (GenBank accession number R15387) and p38γ/SAPK3 [26–27] (GenBank accession number H14292) were obtained from Research Genetics. p38 kinase, p38γ and a constitutively active mutant of MKK6 (MKK6 S207D, T211D) were expressed as amino-terminal His-tagged proteins in *Escherichia coli* and purified by nickel-chelate chromatography using standard protocols (Qiagen). Single amino acid substitutions by alanine or methionine at residue 106 were introduced into p38 by oligonucleotide-directed mutagenesis.

Activation and assay of p38 kinases

For activation, p38, p38γ or p38 mutants (500 nM) were incubated with MKK6 (25 nM) for 30 min at 30°C in a mixture containing 1 mM ATP, 1 mM $MgCl_2$, 1 mM $MnCl_2$, 25 mM HEPES pH 7.5, and 0.1 mM DTT. After activation, p38 kinases were diluted into kinase reaction mix to give the following final concentrations: 100 nM p38, 5 nM MKK6, 200 mM ATP, 8 mM ^{33}P-ATP, 5 mM myelin basic protein, 1 mM $MgCl_2$, 1 mM $MnCl_2$, 25 mM HEPES, pH 7.5, and 0.1 mM DTT. Inhibitors were added to the kinase reaction mix before the addition of p38. After incubation at 30°C for 15–30 min, the reactions were terminated by spotting onto phosphocellulose paper squares which were washed extensively with phosphoric acid, dried, and counted.

Dissociation constant for VK-19911

The fluorescence measurements were obtained on Perkin-Elmer LS 50B fluorimeter. Excitation of p38 (activated or nonactivated) at 280 nm results in emission at 335 nm. Upon VK-19911 binding to p38, a new

Figure 7

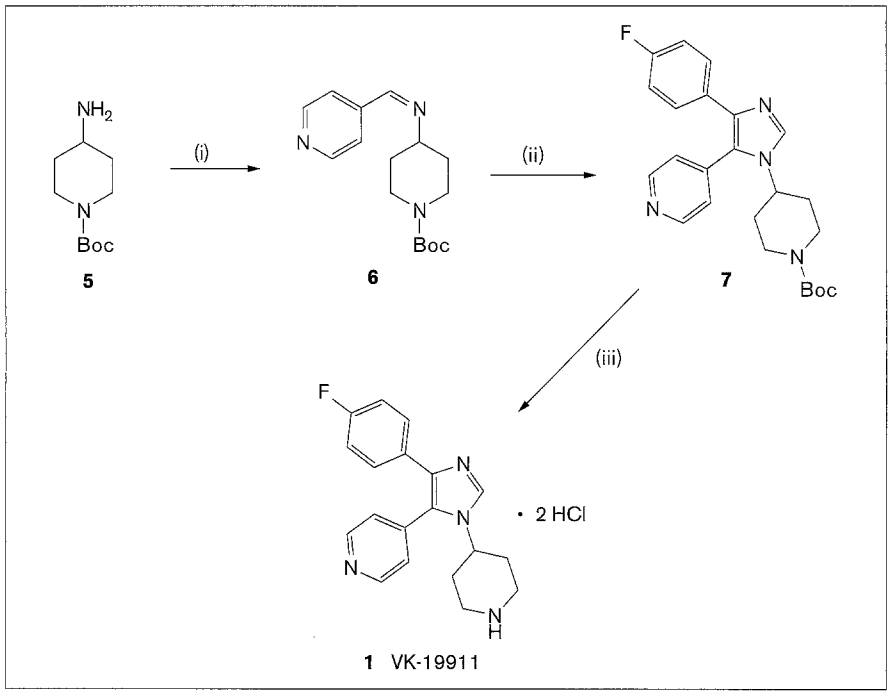

Synthesis of VK-19911. Reagents and conditions: (i) pyridine-4-carboxaldehyde, $MgSO_4$, toluene, 18 h, room temperature; (ii) 4-fluorophenyltolythiomethylisocyanide, 1,5,7-triazabicyclo[4.4.0]dec-5-ene (TBD), methylene chloride; (iii) 4 N HCl/dioxane, 1 h.

emission band appears, centered at 375 nm, with a concomitant decrease in emission at 335 nm. A cuvette of 1 cm path length was placed in the cell compartment with 1.5 ml of 0.1 M HEPES buffer, pH 7.6, containing 10 mM magnesium chloride, 25 mM β-glycerolphosphate and 80 nM p38 (activated or nonactivated). The contents of the cuvette were stirred continuously by the magnetic stirrer in the cell compartment. The excitation and emission wavelengths were set at 280 nm and 375 nm, respectively. A DMSO solution of VK-19911 at 10 μM was added 1 μl at a time without removing the cuvette. The signal at 375 nm was noted as a function of the concentration of VK-19911. The data were fitted to Equation 1 to evaluate the dissociation constant, K_d, for VK-19911.

$$F = 0.5 * EXT * ((K_d + L_0 + E_0) - ((K_d + L_0 + E_0)^2 - 4 * E_0 * L_0)^{1/2}) \quad (1)$$

where F is the observed fluorescence, EXT is the molar fluorescence coefficient, L_0 is VK-19911 concentration, and E_0 is p38 MAP kinase concentration.

Analysis of the bound conformation of VK-19911

To determine the strain energy of the bound state we examined the conformational preferences of VK-19911. The piperidine ring can flip into two distinct chair conformations. In addition, the piperidine, benzene, and pyridine rings all can rotate. *Ab initio* calculations at the Hartree-Fock 6-31G* level were carried out for a series of low-energy conformations using Gaussian-94. First, we determined that the imidazole ring has a 3 kcal/mol preference to adopt an equatorial arrangement with respect to the piperidine ring. Such a strong equatorial preference was expected based on the known 3 kcal/mol preference for equatorial phenylcyclohexane [38]. Next we studied the rotational preferences of the piperidine, pyridine, and benzene rings with respect to the imidazole. All three rotors are fairly 'soft', allowing rotations of ±30° with little energetic penalty. Our calculations reveal that the global energy minimum structure for VK-19911 is similar to the crystallographically observed bound conformation. Furthermore, the calculated energy of the X-ray conformation was only ~1.5 kcal/mol above the global minimum.

Note added in proof

The crystal structure of human p38 MAP kinase in complex with a 2,4,5-triarylimidazole analog of SB-203580 at 2.0 Å resolution was published recently (Tong, L., *et al.*, & Pargellis, C.A. (1997). A highly specific inhibitor of human p38 MAP kinase binds in the ATP pocket. *Nat. Struct. Biol.* 4, 311-316).

Acknowledgements

We thank Xiaoling Xie for providing the ERK2–ATP structure coordinates, and Ted Fox and Joyce Coll for purification of MKK6 and ERK2. We thank Brett O'Hare for oligonucleotide synthesis. We are grateful to F.G. Salituro, V. Sato and J. Boger for their comments on the manuscript.

References

1. Davis, R.J. (1995). Transcriptional regulation by MAP kinases. *Mol. Reprod. Dev.* **42**, 459-467.
2. Cobb, M.H. & Goldsmith, E.J. (1995). How MAP kinases are regulated. *J. Biol. Chem.* **270**, 14843-14846.
3. Bokemeyer, D., Sorokin, A. & Dunn, M.J. (1996). Multiple intracellular MAP kinase signaling cascades. *Kidney Int.* **49**, 1187-1198.
4. Derijard, B., *et al.*, & Davis, R.J. (1994). JNK1: a protein kinase stimulated by UV light and Ha-Ras that binds and phosphorylates the c-Jun activation domain. *Cell* **76**, 1025-1037.
5. Han, J., Lee, J.D., Bibbs, L. & Ulevitch, R.J. (1994). A MAP kinase targeted by endotoxin and hyperosmolarity in mammalian cells. *Science* **265**, 808-811.
6. Raingeaud, J., *et al.*, & Davis, R.J. (1995). Pro-inflammatory cytokines and environmental stress cause p38 mitogen-activated protein kinase activation by dual phosphorylation on tyrosine and threonine. *J. Biol. Chem.* **270**, 7420-7426.
7. Shapiro, L. & Dinarello, C.A., (1995). Osmotic regulation of cytokine synthesis *in vitro*. *Proc. Natl Acad. Sci. USA* **92**, 12230-12234.
8. Derijard, B., *et al.*, & Davis, R.J. (1995). Independent human MAP-kinase signal transduction pathways defined by MEK and MKK isoforms. *Science* **267**, 682-685.
9. Han, J., Lee, J.-D., Jiang, Y., Li, Z., Feng, L. & Ulevitch, R.J. (1996). Characterization of the structure and function of a novel MAP kinase kinase (MKK6). *J. Biol. Chem.* **271**, 2886-2891.

10. Raingeaud, J., Whitmarsh, A.J., Barrett, T., Derijard, B. & Davis, R.J. (1996). MKK3- and MKK6-regulated gene expression is mediated by the p38 mitogen-activated protein kinase signal transduction pathway. *Mol. Cell. Biol.* **16**, 1247-1255.
11. Lee, J.C., *et al.*, & Young, P.R. (1994). A protein kinase involved in the regulation of inflammatory cytokine biosynthesis. *Nature* **372**, 739-746.
12. Cuenda, A., *et al.*, & Lee, J.C. (1995). SB 203580 is a specific inhibitor of a MAP kinase homologue which is stimulated by cellular stresses and interleukin-1. *FEBS Lett.* **364**, 229-233.
13. Cuenda, A., Cohen, P., Buee-Scherrer, V. & Goedert, M. (1997). Activation of stress-activated protein kinase 3 (SAPK3) by cytokines and cellular stresses is mediated via SAPKK3 (MKK6); comparison of the specificities of SAPK3 and SAPK2 (RK/p38). *EMBO J.* **16**, 295-305.
14. Badger, A.M., *et al.*, & Griswold, D.E. (1996). Pharmacologic profile of SB 203580, a selective inhibitor of cytokine suppressive binding protein/p38 kinase, in animal models of arthritis, bone resorption, endotoxin shock and immune function. *J. Pharm. Exp. Therapeut.* **279**, 1453-1461.
15. Saklatvala, J., *et al.*, & Farndale, R.W. (1996). Role for p38 mitogen-activated protein kinase in platelet aggregation caused by collagen of a thromboxane analogue. *J. Biol. Chem.* **271**, 6586-6589.
16. Young, P.R., McDonnell, P., Dennington, D., Hand, A., Laydon, J. & Lee, J.C. (1993). Bicyclic imidazoles inhibit IL-l and TNF production at the protein level. *Agents Actions* **39**, C67-C69.
17. Wang, X., & Ron, D. (1996). Stress-induced phosphorylation and activation of the transcription factor CHOP (GADD153) by p38 MAP kinase. *Science* **272**, 1347-1349.
18. Han, J., Jiang, Y., Li, Z., Kravchenko, V.V. & Ulevitch, R.J. (1997). Activation of the transcription factor MEF2C by the MAP kinase p38 in inflammation. *Nature* **386**, 296-299.
19. Rouse, J., *et al.*, & Nebreda, A.R. (1994). A novel kinase cascade triggered by stress and heat shock that stimulates MAPKAP kinase-2 and phosphorylation of the small heat shock proteins. *Cell* **78**, 1027-1037.
20. McLaughlin, M.M., *et al.*, & Young, P.R. (1996). Identification of mitogen-activated protein (MAP) kinase-activated protein kinase-3, a novel substrate of CSBP p38 MAP kinase. *J. Biol. Chem.* **271** (14) 8488-8492.
21. Guan, Z., Baier, L.D. & Morrison, A.R. (1997). p38 mitogen-activated protein kinase down-regulates nitric oxide and up-regulates prostaglandin E2 biosynthesis stimulated by Interleukin-1β. *J. Biol. Chem.* **272**, 8083-8089.
22. Xia, Z., Dickens, M., Raingeaud, J., Davis, R.J. & Greenberg, M.E. (1995). Opposing effects of ERK and JNK-p38 MAP kinases on apoptosis. *Science* **270**, 1326-1331.
23. Wilson, K.P, *et al.*, & Su, M.S.S. (1996). Crystal structure of p38 mitogen-activated protein kinase. *J. Biol. Chem.* **271**, 27696-27700.
24. Wang, Z., Harkins, P.C., Ulevitch, R.J., Han, J., Cobb, M.H. & Goldsmith, E.J. (1997). The structure of mitogen-activated protein kinase p38 at 2.1 Å resolution. *Proc. Natl. Acad. Sci. USA* **94**, 2327-2332.
25. Zhang, F., Strand, A., Robbins, D., Cobb, M.H. & Goldsmith, E.J. (1994). Atomic structure of the MAP kinase ERK2 at 2.3 Å resolution. *Nature* **367**, 704-711.
26. Gallagher, T.F., *et al.*, & Adams, J.L. (1997). Regulation of stress-induced cytokine production by pyridinylimidazoles; inhibition of CSBP kinase. *Bioorg. Med. Chem.* **5**, 49-64.
27. Li, Z., Jiang, V., Ulevitch, R.J. & Han, J. (1996). The primary structure of p38 gamma: a new member of the p38 group of MAP kinases. *Biochem. Biophys. Res. Commun.* **228**, 334-340.
28. Mertens, S., Craxton, M. & Goedert, M. (1996). SAP kinase-3, a new member of the family of mammalian stress-activated protein kinases. *FEBS Lett* **383**, 273-276.
29. Johnson, L.N., Noble, M.E.M. & Owen, D.J. (1996). Active and inactive protein kinases: structural basis for regulation. *Cell* **85**, 149-158.
30. Doza, Y.N., Cuenda, A., Thomas, G.M., Cohen, P. & Nebreda, A.R. (1995). Activation of the MAP kinase homologue RK requires the phosphorylation of Thr180 and Tyr182 and both residues are phosphorylated in chemically stressed KB cells. *FEBS Lett.* **364**, 223-228.
31. Gallagher, T.F., *et al.*, & Adams, J.L. (1995). 2,4,5-triarylimidazole inhibitors of IL-1 biosynthesis. *Bioorg. Med. Chem. Lett.* **5**, 1171-1176.
32. Boehm, J.C., *et al.*, & Adams, J.L. (1996). 1-Substituted 4-aryl-5-pyridinylimidazoles: a new class of cytokine suppressive drugs with low 5-lipoxygenase and cyclooxygenase inhibitory potency. *J. Med. Chem.* **39**, 3929-3937.
33. Van Leusen, A.M., Wildeman, J. & Oldenziel, O.H. (1977). Base-induced cycloaddition of sulfonylmethyl isocyanides to C,N double bonds. Synthesis of 1,5-disubstituted and 1,4,5-trisubstituted imidazoles from aldimines and imidoyl chlorides. *J. Org. Chem.* **42**, 1153-1159.
34. Adams, Sheldiake, Gallagher, Garigipati; SmithKline Beecham US 08092,733 (CIP); International Publication Number: WO 95/02591.
35. Mach, R.H., *et. al.*, & Evora, P.H. (1993). 18F-labeled benzamides for studying the dopamine D2 receptor with positron emission tomography. *J. Med. Chem.* **36**, 3707-3719.
36. Otwinowski, Z., & Minor, W. (1996). Processing of X-ray diffraction data collected in oscillation mode. In *Methods in Enzymology* (Carter, C.W. & Sweet, R.M., Eds), Academic Press. New York, USA.
37. Brünger, A.T. (1992). XPLOR: *A System for X-ray Crystallography and NMR.* (Yale University Press, New Haven, CT, USA) Version 3.1.
38. Burkert, U. & Allinger, N.L. (1982) In *Molecular Mechanics*, American Chemical Society Monograph No. 177, ACS Press, Washington, DC, USA.